Sample pages from "Optical Measurement of Surface Topography"
Full document available from Springer Verlag

8 Phase Shifting Interferometry

Peter de Groot

Zygo Corporation
Laurel Brook Road
Middlefield, Connecticut, USA

Abstract. Phase shifting interferometry is a well-established technique for areal surface characterisation that relies on digitisation of interference data acquired during a controlled phase shift, most often introduced by controlled mechanical oscillation of an interference objective. The technique provides full 3D images with typical height measurement repeatability of less than 1 nm independent of field size. Microscopes for interferometry employ a range of specialised interference objectives for roughness and microscopic form measurement.

8.1 Concept and Overview

From the earliest days of measuring microscopy, it was understood that a reference reflection superimposed on the object reflection would generate fringes of interference that relate to surface topography. Perhaps the simplest interference instrument is an ordinary, non-interferometric microscope observing an object with a cover slip positioned close to the object surface, to provide the necessary reference reflection. In ordinary white light illumination, the resulting Fizeau interference fringes are multi-coloured and have the strongest contrast when the cover slip is almost in physical contact with the object surface. The shapes of the fringes (straight, circular, irregular) are indicative of the surface shape. Microscopes specifically designed for interferometry employ a specialised objective with an internal beam-splitter and reference allowing convenient optical contact with a large physical working distance to the object. Such microscopes also often make use of a narrow-band filter or near-monochromatic light source to improve the fringe contrast over a wide range of measurement conditions.

Modern interference microscopes generally employ image detection using an electronic camera and computer analysis for convenience, measurement accuracy and automation. From 1980 to 1990, there were significant developments of these automated 3D measuring microscopes using the principles of phase shifting interferometry (PSI), first developed in the context of optical testing of lenses and mirrors. PSI acquires a sequence of images with a precisely controlled phase change

Sample pages from "Optical Measurement of Surface Topography"
Full document available from Springer Verlag

between them, which when a few fringes are visible on the surface, manifests itself as a shift in fringe position between the images captured by a camera. The phase shifting is almost always generated by a mechanical motion of the interference objective, which allows for fast, non-contact metrology.

This chapter discusses the most common forms of interference microscopy for 3D surface measurement using an internal reference mirror. The common feature of PSI instruments is that, unlike differential or phase contrast methods, surface heights are directly proportional to interference phase.

8.2 Principles of Surface Measurement Interferometry

Interferometers take advantage of the wave properties of light to analyse surface characteristics, including in particular surface height variations. For evaluation of areal surface topography, interferometers separate source light so that it follows two independent paths, one of which includes a reference surface and the other the object surface. The separated light beams then recombine and are directed to a digital camera that measures the resultant light intensity over multiple image points simultaneously. The intensity of the recombined light exhibits high sensitivity to the differences in path lengths, effectively comparing the object surface with the reference surface with nanometre resolution.

The interference phenomenon may be understood by considering the classical Michelson interferometer shown in Fig. 8.1, here assumed equipped with a high-coherence light source such as a laser. Following the usual two-beam interference analysis (see for example Hariharan 1992), the interference signal observed at the square-law detector can be written

$$I(h,\zeta) = I_{DC} + I_{AC}\cos\left[K(h-\zeta)+\xi\right], \tag{8.1}$$

where I_{DC} and $I_{AC} < I_{DC}$ are fixed coefficients. The quantity

$$K = 4\pi/\lambda\,, \tag{8.2}$$

sometimes called the fringe frequency, corresponds to the rate at which the interference signal oscillates sinusoidally as a function of changes in sample surface height h or in position ζ of the reference mirror. In equation (8.2), λ is the source wavelength and ξ is a phase offset related to the reflection and transmission properties of the interferometer components. The inset graph in Fig. 8.1 shows the variation in detected intensity as a function of the difference $h-\zeta$. The periodic modulations are characteristic of interference phenomena, with a full cycle of modulation every half wavelength of motion of the reference mirror.

Sample pages from "Optical Measurement of Surface Topography"
Full document available from Springer Verlag

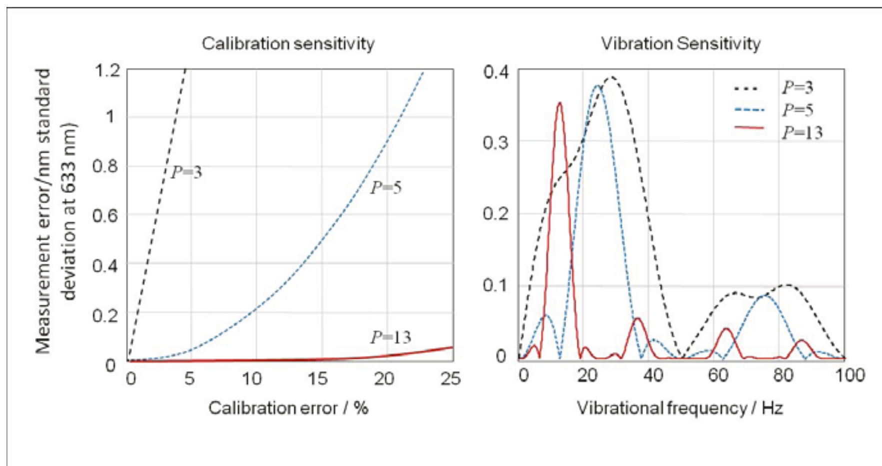

Fig. 8.4 PSI calibration sensitivity (left) vibrational sensitivity (right) for the first three algorithms in Table 8.1

8.6 Interferometer Design

The history of interferometric methods for characterisation of microscopic objects has been previously reviewed by Krug et al. (1964) and by Pluta (1993). The range of instrumentation for interference microscopy extends from the simple addition of a reference surface directly, to the object to the elaboration of complex, dedicated platforms employing variations of all known methods for division of wavefront and for division of amplitude adapted to high magnification instruments.

Modern interference microscopes have evolved to instrument platforms recognizable as refined versions of a conventional microscope, configured for digital data acquisition and low vibration, combined with one or more removable interference objectives that take the place of the conventional imaging microscope objective. This basic design provides flexibility and convenience, allowing the use of a turret of interference objectives of varying magnification and interferometer design depending on the needs of the application.

Fig. 8.5 illustrates the optical configuration of a microscope for interchangeable interference objectives, using a common interferometer design derived from the modified Michelson geometry of Fig. 8.2. Within the objective, a beam-splitter placed between the imaging optics and the sample establishes the reference and measurement paths. The beam-splitter is most often a prism. Variants of the basic design include those with fixed or adjustable dispersion compensation for use with samples having a transparent glass cover (Hedley 2001, Han 2006).

The system magnification is determined by the ratio of the tube lens focal length to the focal length of the objective. The objective magnification is defined in terms of a nominal unity-magnification tube lens focal length, which varies between 160 mm and 200 mm, depending on the manufacturer. Thus a 10× objective for a defined 200 mm tube lens has a focal length of 20 mm.

Sample pages from "Optical Measurement of Surface Topography"
Full document available from Springer Verlag

The working distance from the objective housing to the object is a function of the design of the objective, and relates to factors such as interferometer geometry, focal length, mechanical structure and lens design. A large working distance is generally preferred and can be a deciding factor in the choice of interferometer geometry.

At higher magnifications, usually for 20× and above, there is insufficient working distance to accommodate a large beam-splitter between the objective lens and the sample and the Michelson geometry is no longer practical. Fig. 8.6 shows a Mirau objective with a parallel beam-splitter and reference surface, both aligned with the optical axis of the imaging lenses (Mirau 1952). The reference is a small reflective disk, somewhat larger in diameter than the field of view of the objective, and typically comprised of a coating on an otherwise transparent supporting plate of identical thickness to the beam-splitter. The design inherently relies on a sufficiently large numerical aperture (see Chapter 2) to allow at least a portion of the illuminating and imaging rays to pass around the reflecting reference disk, often referred to as the central obscuration. The Mirau is by far the most common high-magnification interference objective in use today.

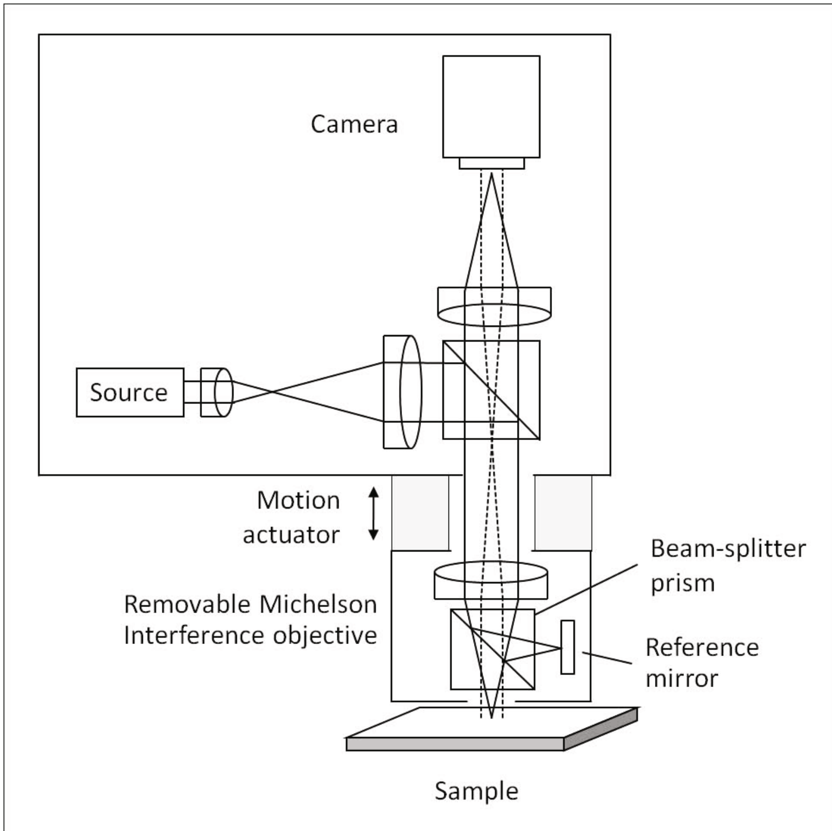

Fig. 8.5 Interferometer for areal surface measurement employing a Michelson-type interference objective

Sample pages from "Optical Measurement of Surface Topography"
Full document available from Springer Verlag

fine surface detail. Often referred to as lateral resolution, this performance specification for interference microscopes varies significantly with magnification and can have a strong effect on the perceived variations in surface height, particularly for roughness (see Chapter 2).

An informative method of describing the lateral resolving power of interference microscopes is by the instrument transfer function (ITF) (Takacs 1993, de Groot and Colonna de Lega 2006). The ITF describes how the instrument would respond to an object surface having a specific spatial frequency. The ITF is the 3D measurement analogy to the more conventional optical transfer function (OTF), the latter referring to an optical instrument's ability to generate 2D images.

The ITF tells us what the measured amplitude of a sinusoidal grating of a specified spatial frequency ν (in lines per millimetre) would be relative to the true amplitude of the sinusoid. In the limit of very small surface heights, the magnitude of the ITF for a PSI instrument is the same as the more familiar modulation transfer function (MTF). Using the result for the OTF, the ITF of a PSI instrument having an incoherent light source that fills the objective pupil is

$$\mathrm{ITF}(\nu) = \frac{2}{\pi}\left[\phi - \cos(\phi)\sin(\phi)\right] \tag{8.13}$$

where

$$\phi = \arccos\left(\frac{\lambda \nu}{2A_N}\right). \tag{8.14}$$

This ITF must be multiplied by the MTF of the camera, which has limited resolution related to pixel size. Fig. 8.8 shows the ITF for 5×, 20× and 100× microscope objectives (numerical aperture A_N equal to 0.13, 0.3 and 0.8, respectively).

Setting aside the contribution of the camera resolution, the ITF reaches zero for a spatial frequency given by $\phi = 0$ or

$$\nu_{0\%} = \frac{2A_N}{\lambda}, \tag{8.15}$$

which is the Sparrow criterion for optical resolution. The 50 % point is at

$$\nu_{50\%} = \frac{A_N}{1.22\lambda}, \tag{8.16}$$

which is approximately half the spatial frequency (twice the spatial period) of the Rayleigh criterion (Smith 1966, see also Chapter 2). Tab. 8.2 summarises the optical lateral resolution for common PSI objectives in terms of these two criteria.

Sample pages from "Optical Measurement of Surface Topography"
Full document available from Springer Verlag

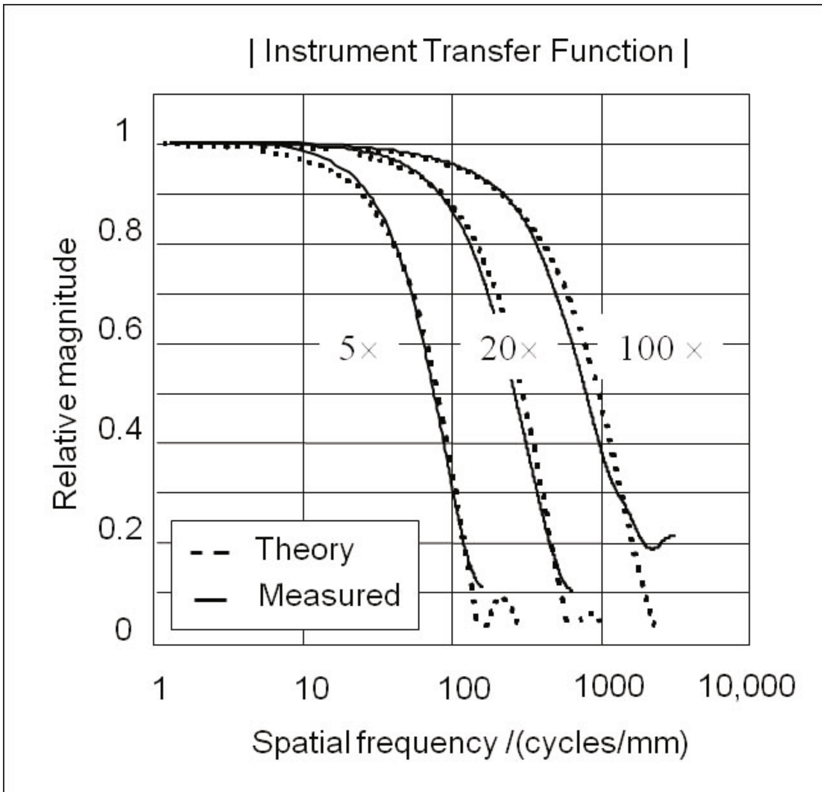

Fig. 8.8 Measured and theoretical magnitude of the ITF

Table 8.2 Optical lateral resolution of common interference objectives, assuming perfect optics

Magnification	A_N	Raleigh / µm	Sparrow / µm
1×	0.03	11.18	9.17
2.5×	0.08	4.47	3.67
5×	0.13	2.58	2.12
10×	0.30	1.12	0.92
20×	0.40	0.84	0.69
50×	0.55	0.61	0.50
100×	0.80	0.42	0.34

Camera resolution is usually matched to the optical resolution up to a magnification of approximately 10×, meaning that the pixel size in object space has the same lateral dimensions as listed in Tab. 8.2. Above a magnification of 20×, the camera resolution exceeds the optical resolution, becoming a negligible limit on the net ITF at 100×, as is apparent from Fig. 8.8.

However, having a particular numerical aperture does not mean that the objective will perform as tabulated in Table 8.2. Aberrations, focus errors or variations

Sample pages from "Optical Measurement of Surface Topography"
Full document available from Springer Verlag

de Groot, P., Colonna de Lega, X.: Interpreting interferometric height measurements using the instrument transfer function. In: Proc. FRINGE 2005, pp. 30–37. Springer, Berlin (2006)
de Groot, P.: Design of error-compensating algorithms for sinusoidal phase shifting interferometry. Appl. Opt. 48, 6788–6796 (2009)
Dubois, A.: Phase-map measurements by interferometry with sinusoidal phase modulation and four integrating buckets. J. Opt. Soc. Am. A 18, 1972–1979 (2001)
Freischlad, K., Koliopoulos, C.L.: Fourier description of digital phase-measuring interferometry. J. Opt.Soc. Am. A 7, 542–551 (1990)
Greivenkamp, J.E.: Generalized data reduction for heterodyne interferometry. Opt. Eng. 23, 350–352 (1984)
Greivenkamp, J.E., Bruning, J.H.: Phase shifting interferometry. In: Malacara, D. (ed.) Optical shop testing, 2nd edn. John Wiley & Sons, Hoboken (1992)
Han, S.: Interferometric testing through transmissive media (TTM). In: Proc. SPIE, vol. 6293, pp. 629301–629305 (2006)
Hariharan, P.: Basics of interferometry. Academic Press, London (1992)
Hedley, J., Harris, A., Burdess, J., McNie, M.: The Development of a workstation for optical testing and modification of IMEMS on a wafer. In: Proc. SPIE, vol. 4408, pp. 402–408 (2001)
Koliopoulos, C.: Interferometric optical phase measurement techniques. University of Arizona, PhD Thesis (1981)
Krug, W., Rienitz, J., Schulz, G.: Contributions to interference microscopy. Hilger & Watts Ltd (1964)
Lai, G., Yatagai, T.: Generalized phase-shifting interferometry. J. Opt. Soc. Am. A 8, 822–827 (1991)
Linnik, V.P.: Ein apparat fur mikroskopisch-interferometrische untersuchung reflektierender objekte (mikrointerferometer). Akademiya Nauk S.S.S.R. Doklady (1933)
Malacara, D., Servin, M., Malacara, Z.: Interferogram analysis for optical testing. Marcel Dekker, New York (1998)
Massig, J.H.: Interferometric profilometer sensor. US Patent 5,166,751 (1992)
Mirau, A.H.: Interferometer. US Patent 2,612,074 (1952)
Pluta, M.: Advanced light microscopy, vol. 3. Elsevier, Amsterdam (1993)
Sasaki, O., Okazaki, H., Sakai, M.: Sinusoidal phase modulating interferometer using the integrating-bucket method. Appl. Opt. 26, 1089–1093 (1987)
Schmit, J., Creath, K., Wyant, J.C., Malacara, D.: Optical shop testing. In: Malacara, D. (ed.) Surface profilers, multiple wavelength and white light interferometry, 3rd edn., ch. 15, pp. 667–755. John Wiley & Sons, Hoboken (2007)
Schreiber, H., Bruning, J.H.: Phase shifting interferometry. In: Malacara, D. (ed.) Optical Shop Testing, 3rd edn. John Wiley & Sons, Hoboken (2007)
Schwider, J., Burow, R., Elssner, K.-E., Grzanna, J., Spolaczyk, R., Merkel, K.: Digital wave-front measuring interferometry: some systematic error sources. Appl. Opt. 22, 3421–3432 (1983)
Smith, W.J.: Modern optical engineering, p. 139. McGraw-Hill, New York (1966)
Sommargren, G.E.: Optical heterodyne profilometry. Appl. Opt. 20, 610–618 (1981)
Surrel, Y.: Design of algorithms for phase measurements by the use of phase stepping. Appl. Opt. 35, 51–60 (1996)
Takacs, S.P., Li, M., Furenlid, K., Church, E.: A step-height standard for surface profiler calibration. In: Proc. SPIE, vol. 235, pp. 65–74 (1993)
Takeda, M., Hideki, I., Kobayashi, S.: Fourier-ransform method of fringe-pattern analysis for computer based topography and tnterferometry. J. Opt. Soc. Am. 72, 156–160 (1982)
Wyant, J.C., Koliopoulos, C.L., Bushan, B., George, O.E.: An optical profilometer for surface characterization of magnetic media. ASLE Trans. 27, 101 (1984)